УДК 539.3
DOI: 10.17277/vestnik.2020.02.pp.306-322

COUPLED THERMO-ELECTRO-MECHANICAL ANALYSIS OF HYBRID LAYERED CYLINDRICAL SHELLS WITH PIEZOELECTRIC SENSORS AND ACTUATORS

G. M. Kulikov, N. P. Merkusheva, M. G. Kulikov, S. V. Plotnikova

Laboratory of Intelligent Materials and Structures, gmkulikov@mail.ru;
Tambov State Technical University, Tambov, Russia

Keywords: layered piezoelectric shell; thermopiezoelectricity; 3D stress analysis; sampling surfaces method.

Abstract: This paper focuses on the implementation of the sampling surfaces (SaS) method for solving the three-dimensional coupled problems for layered piezoelectric shells subjected to thermal and electromechanical loading. The SaS method is based on choosing inside the *n*th layer I_n SaS parallel to the middle surface in order to introduce the temperatures, electric potentials and displacements of these surfaces as basic unknowns. Such choice of unknowns with the consequent use of the Lagrange polynomials of degree $I_n - 1$ in assumed approximations of the temperature, electric potential, displacements and mechanical material properties through the thickness of the layer leads to an efficient thermopiezoelectric shell model. The inner SaS are located inside each layer at Chebyshev polynomial nodes that allows one to minimize uniformly the error due to the Lagrange interpolation of high order. As a result, the SaS method can be applied efficiently for obtaining the analytical solutions for hybrid layered cylindrical shells with piezoelectric sensors and actuators, which asymptotically approach the exact solutions of thermopiezoelectricity as the number of SaS I_n tends to infinity.

Introduction

Three-dimensional (3D) analysis of layered piezoelectric plates and shells under thermal loading has received considerable attention during past twenty years (see, e.g. [1, 2]). There are at least five approaches to 3D exact solutions of thermoelectroelasticity for piezoelectric plates and shells, namely, the Pagano approach [3 – 7], the state space approach [8 – 12], the power series expansion approach [13 – 15], the asymptotic expansion approach [16], and the sampling surfaces (SaS) approach [17 – 19].

In this paper, the SaS approach is utilized for the first time for the coupled thermoelectroelastic stress analysis of hybrid layered composite shells with piezoelectric sensors and actuators. According to the SaS approach [20], we choose arbitrarily located surfaces inside the *n*th layer parallel to the middle surface of a shell $\Omega^{(n)1}, \Omega^{(n)2}, ..., \Omega^{(n)I_n}$ to introduce temperatures $T^{(n)1}, T^{(n)2}, ..., T^{(n)I_n}$, electric potentials $\varphi^{(n)1}, \varphi^{(n)2}, ..., \varphi^{(n)I_n}$ and displacement vectors $\mathbf{u}^{(n)1}, \mathbf{u}^{(n)2}, ..., \mathbf{u}^{(n)I_n}$ of these surfaces as basic shell variables, where I_n is the total number of SaS of the *n*th layer ($I_n \geq 3$). Such choice of temperatures, electric potentials and displacements with the consequent use of the Lagrange polynomials of degree $I_n - 1$ in the assumed distributions of the temperature, electric potential, displacements and mechanical properties through the thickness of the layer allows the presentation of governing equations of the SaS shell formulation in a very compact form.

It should be noted that the SaS shell formulation with equally spaced SaS [21 – 23] does not work properly with the Lagrange polynomials of high degree because of Runge's phenomenon [24]. This phenomenon yields the wild oscillation at the edges of the interval when the user deals with some specific functions similar to the shell metric functions. If the number of equispaced nodes is increased then the oscillations become even larger. However, the use of the Chebyshev polynomial nodes inside the shell body [20, 25, 26] can help to improve significantly the behavior of the Lagrange polynomials of high degree because such a choice permits one to minimize uniformly the error due to the Lagrange interpolation. This fact gives an opportunity to obtain the stresses with a prescribed accuracy using the sufficiently large number of SaS. It means in turn that the solutions based on the SaS concept *asymptotically* approach the 3D exact solutions of thermoelectroelasticity as $I_n \to \infty$.

Description of displacement and strain fields

We consider a layered shell of the thickness *h*. Let the middle surface Ω be described by orthogonal curvilinear coordinates θ_1 and θ_2, which are referred to the lines of principal curvatures of its surface. The thickness coordinate θ_3 is oriented in the normal direction. Introduce the following notations: $A_\alpha(\theta_1, \theta_2)$ are the coefficients of the first fundamental form; $k_\alpha(\theta_1, \theta_2)$ are the principal curvatures of the middle surface; $c_\alpha = 1 + k_\alpha \theta_3$ are the components of the shifter tensor; $c_\alpha^{(n)i_n}(\theta_1, \theta_2)$ are the components of the shifter tensor at SaS of the *n*th layer $\Omega^{(n)i_n}$ (Fig. 1) defined as

$$c_\alpha^{(n)i_n} = c_\alpha(\theta_3^{(n)i_n}) = 1 + k_\alpha \theta_3^{(n)i_n}, \tag{1}$$

where $\theta_3^{(n)i_n}$ are the transverse coordinates of SaS given by

$$\theta_3^{(n)1} = \theta_3^{[n-1]}, \quad \theta_3^{(n)I_n} = \theta_3^{[n]},$$

$$\theta_3^{(n)m_n} = \frac{1}{2}(\theta_3^{[n-1]} + \theta_3^{[n]}) - \frac{1}{2} h^{(n)} \cos\left(\pi \frac{2m_n - 3}{2(I_n - 2)}\right), \tag{2}$$

where $\theta_3^{[n-1]}$ and $\theta_3^{[n]}$ are the transverse coordinates of layer interfaces $\Omega^{[n-1]}$ and $\Omega^{[n]}$; $h^{(n)} = \theta_3^{[n]} - \theta_3^{[n-1]}$ is the thickness of the *n*th layer. It is worth noting that the transverse coordinates of inner SaS $\theta_3^{(n)m_n}$ coincide with the coordinates of the Chebyshev polynomial nodes. This fact has a great meaning for the convergence of the SaS method [20].

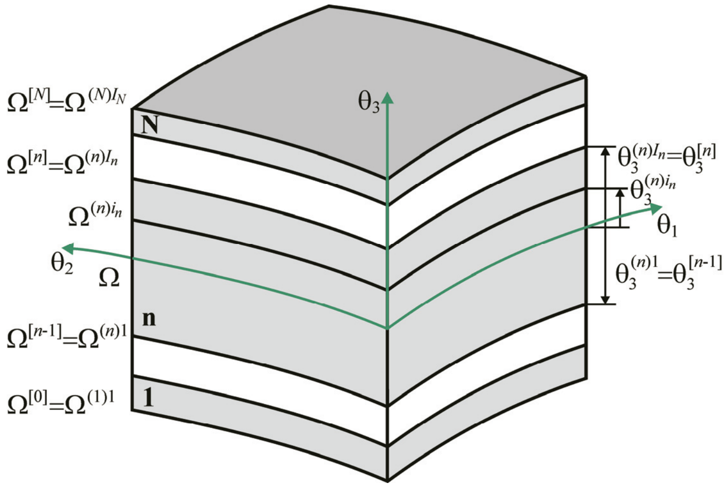

Fig. 1. Geometry of the layered shell

Here, the index n identifies the belonging of any quantity to the nth layer and runs from 1 to N, where N is the number of layers; the index m_n identifies the belonging of any quantity to the inner SaS of the nth layer and runs from 2 to $I_n - 1$; the indices i_n, j_n, k_n describe all SaS of the nth layer and run from 1 to I_n; Latin tensorial indices i, j, k, l range from 1 to 3; Greek indices α, β range from 1 to 2.

We start now with the first two assumptions of the proposed layered piezoelectric shell formulation. The displacement and strain fields are distributed through the thickness of the nth layer [20] as follows:

$$u_i^{(n)} = \sum_{i_n} L^{(n)i_n} u_i^{(n)i_n}, \quad \theta_3^{[n-1]} \le \theta_3 \le \theta_3^{[n]}, \tag{3}$$

$$\varepsilon_{ij}^{(n)} = \sum_{i_n} L^{(n)i_n} \varepsilon_{ij}^{(n)i_n}, \quad \theta_3^{[n-1]} \le \theta_3 \le \theta_3^{[n]}, \tag{4}$$

where $u_i^{(n)i_n}(\theta_1, \theta_2)$ and $\varepsilon_{ij}^{(n)i_n}(\theta_1, \theta_2)$ are the displacements and strains of SaS of the nth layer $\Omega^{(n)i_n}$; $L^{(n)i_n}(\theta_3)$ are the Lagrange polynomials of degree $I_n - 1$ given by

$$u_i^{(n)i_n} = u_i(\theta_3^{(n)i_n}), \tag{5}$$

$$\varepsilon_{ij}^{(n)i_n} = \varepsilon_{ij}(\theta_3^{(n)i_n}), \tag{6}$$

$$L^{(n)i_n} = \prod_{j_n \ne i_n} \frac{\theta_3 - \theta_3^{(n)j_n}}{\theta_3^{(n)i_n} - \theta_3^{(n)j_n}}. \tag{7}$$

The strains of SaS of the nth layer in terms of displacements of SaS are expressed as

$$2\varepsilon_{\alpha\beta}^{(n)i_n} = \frac{1}{c_\beta^{(n)i_n}} \lambda_{\alpha\beta}^{(n)i_n} + \frac{1}{c_\alpha^{(n)i_n}} \lambda_{\beta\alpha}^{(n)i_n},$$

$$2\varepsilon_{\alpha 3}^{(n)i_n} = \frac{1}{c_\alpha^{(n)i_n}} \lambda_{3\alpha}^{(n)i_n} + \beta_\alpha^{(n)i_n}, \quad \varepsilon_{33}^{(n)i_n} = \beta_3^{(n)i_n}, \tag{8}$$

where $\lambda_{i\alpha}^{(n)i_n}$ are the strain parameters of SaS of the *n*th layer [20]; $\beta_i^{(n)i_n} = u_{i,3}(\theta_3^{(n)i_n})$ are the values of the derivative of displacements with respect to the thickness coordinate on SaS defined as

$$\lambda_{\alpha\alpha}^{(n)i_n} = \frac{1}{A_\alpha} u_{\alpha,\alpha}^{(n)i_n} + B_\alpha u_\beta^{(n)i_n} + k_\alpha u_3^{(n)i_n}, \quad \lambda_{\beta\alpha}^{(n)i_n} = \frac{1}{A_\alpha} u_{\beta,\alpha}^{(n)i_n} - B_\alpha u_\alpha^{(n)i_n},$$

$$\lambda_{3\alpha}^{(n)i_n} = \frac{1}{A_\alpha} u_{3,\alpha}^{(n)i_n} - k_\alpha u_\alpha^{(n)i_n} \text{ for } \beta \neq \alpha, \tag{9}$$

$$\beta_i^{(n)i_n} = \sum_{j_n} M^{(n)j_n}(\theta_3^{(n)i_n}) u_i^{(n)j_n}, \tag{10}$$

where $M^{(n)j_n} = L_{,3}^{(n)j_n}$ are the derivatives of Lagrange polynomials; their values on SaS are calculated as

$$M^{(n)j_n}(\theta_3^{(n)i_n}) = \frac{1}{\theta_3^{(n)j_n} - \theta_3^{(n)i_n}} \prod_{k_n \neq i_n, j_n} \frac{\theta_3^{(n)i_n} - \theta_3^{(n)k_n}}{\theta_3^{(n)j_n} - \theta_3^{(n)k_n}} \text{ for } j_n \neq i_n,$$

$$M^{(n)i_n}(\theta_3^{(n)i_n}) = -\sum_{j_n \neq i_n} M^{(n)j_n}(\theta_3^{(n)i_n}). \tag{11}$$

It is seen from formula (10) that the key functions $\beta_i^{(n)i_n}$ of the layered shell formulation are represented as a linear combination of displacements of SaS of the *n*th layer $u_i^{(n)j_n}$.

Description of electric field

Next, we introduce the third and fourth assumptions of the proposed layered thermopiezoelectric shell formulation. The electric potential and the electric field are distributed through the thickness of the *n*th layer [18] as follows:

$$\varphi^{(n)} = \sum_{i_n} L^{(n)i_n} \varphi^{(n)i_n}, \quad \theta_3^{[n-1]} \leq \theta_3 \leq \theta_3^{[n]}, \tag{12}$$

$$E_i^{(n)} = \sum_{i_n} L^{(n)i_n} E_i^{(n)i_n}, \quad \theta_3^{[n-1]} \leq \theta_3 \leq \theta_3^{[n]}, \tag{13}$$

where $\varphi^{(n)i_n}(\theta_1, \theta_2)$ are the electric potentials of SaS of the *n*th layer; $E_i^{(n)i_n}(\theta_1, \theta_2)$ are the components of the electric field at SaS of the *n*th layer defined as

$$\varphi^{(n)i_n} = \varphi(\theta_3^{(n)i_n}), \tag{14}$$

$$E_i^{(n)i_n} = E_i(\theta_3^{(n)i_n}). \tag{15}$$

The electric field on SaS of the *n*th layer in terms of electric potentials of SaS is given by

$$E_{\alpha}^{(n)i_n} = -\frac{1}{A_{\alpha} c_{\alpha}^{(n)i_n}} \varphi_{,\alpha}^{(n)i_n}, \tag{16}$$

$$E_3^{(n)i_n} = -\sum_{j_n} M^{(n)j_n}(\theta_3^{(n)i_n}) \varphi^{(n)j_n}. \tag{17}$$

As can be seen from formula (17), the normal components of the electric field on SaS of the *n*th layer $E_3^{(n)i_n}$ are represented as a linear combination of electric potentials of SaS of the same layer $\varphi^{(n)j_n}$.

Description of temperature field

The following step consists in a choice of the suitable approximation of the temperature and temperature gradient through the shell thickness. The temperature and temperature gradient are distributed through the thickness of the *n*th layer [18] as follows:

$$T^{(n)} = \sum_{i_n} L^{(n)i_n} T^{(n)i_n}, \quad \theta_3^{[n-1]} \le \theta_3 \le \theta_3^{[n]}, \tag{18}$$

$$\Gamma_i^{(n)} = \sum_{i_n} L^{(n)i_n} \Gamma_i^{(n)i_n}, \quad \theta_3^{[n-1]} \le \theta_3 \le \theta_3^{[n]}, \tag{19}$$

where $T^{(n)i_n}(\theta_1, \theta_2)$ are the temperatures of SaS of the *n*th layer; $\Gamma_i^{(n)i_n}(\theta_1, \theta_2)$ are the components of the temperature gradient on SaS of the *n*th layer defined as

$$T^{(n)i_n} = T(\theta_3^{(n)i_n}), \tag{20}$$

$$\Gamma_i^{(n)i_n} = \Gamma_i(\theta_3^{(n)i_n}). \tag{21}$$

The components of the temperature gradient on SaS of the *n*th layer in terms of temperatures of SaS [18] are expressed as

$$\Gamma_{\alpha}^{(n)i_n} = \frac{1}{A_{\alpha} c_{\alpha}^{(n)i_n}} T_{,\alpha}^{(n)i_n}, \tag{22}$$

$$\Gamma_3^{(n)i_n} = \sum_{j_n} M^{(n)j_n}(\theta_3^{(n)i_n}) T^{(n)j_n}. \tag{23}$$

It is seen from formula (23) that the normal components of the temperature gradient at SaS of the *n*th layer $\Gamma_3^{(n)i_n}$ are represented as a linear combination of temperatures of SaS of the same layer $T^{(n)j_n}$.

Constitutive equations

As constitutive equations, we accept Fourier heat conduction equations

$$q_i^{(n)} = -k_{ij}^{(n)} \Gamma_j^{(n)}, \quad \theta_3^{[n-1]} \le \theta_3 \le \theta_3^{[n]}, \tag{24}$$

where $q_i^{(n)}$ are the components of the heat flux of the *n*th layer; $k_{ij}^{(n)}$ are the thermal conductivities. Here and below, the summation on repeated Latin indices is implied.

We introduce the next assumption of the thermal shell formulation. Let us assume that the thermal conductivity coefficients are distributed through the thickness of the nth layer as follows:

$$k_{ij}^{(n)} = \sum_{i_n} L^{(n)i_n} k_{ij}^{(n)i_n}, \quad \theta_3^{[n-1]} \le \theta_3 \le \theta_3^{[n]} \tag{25}$$

that is extensively utilized in this paper, where $k_{ij}^{(n)i_n} = k_{ij}^{(n)}\left(\theta_3^{(n)i_n}\right)$ are the values of the thermal conductivity tensor on SaS of the nth layer.

For simplicity, we consider the case of linear piezoelectric materials. Therefore, the constitutive equations are expressed as

$$\sigma_{ij}^{(n)} = C_{ijkl}^{(n)} \varepsilon_{kl}^{(n)} - e_{kij}^{(n)} E_k^{(n)} - \gamma_{ij}^{(n)} \Theta^{(n)},$$

$$D_i^{(n)} = e_{ikl}^{(n)} \varepsilon_{kl}^{(n)} + \in_{ik}^{(n)} E_k^{(n)} + r_i^{(n)} \Theta^{(n)},$$

$$\eta^{(n)} = \gamma_{kl}^{(n)} \varepsilon_{kl}^{(n)} + r_k^{(n)} E_k^{(n)} + \chi^{(n)} \Theta^{(n)}, \tag{26}$$

where $\sigma_{ij}^{(n)}$ are the stresses of the nth layer; $D_i^{(n)}$ are the electric displacements; $\eta^{(n)}$ is the entropy density; $\Theta^{(n)} = T^{(n)} - T_0$ is the temperature rise; T_0 is the reference temperature; $C_{ijkl}^{(n)}$ are the elastic constants; $e_{kij}^{(n)}$ are the piezoelectric constants; $\gamma_{ij}^{(n)}$ are the thermal stress coefficients; $\in_{ik}^{(n)}$ are the dielectric constants; $r_i^{(n)}$ are the pyroelectric constants; $\chi^{(n)}$ is the entropy-temperature coefficient given by

$$\chi^{(n)} = \rho^{(n)} c_{\mathrm{V}}^{(n)} / T_0, \tag{27}$$

where $\rho^{(n)}$ and $c_{\mathrm{V}}^{(n)}$ are the mass density and the specific heat per unit mass.

Finally, we introduce the last assumption of the SaS thermopiezoelectric shell formulation. Let the material constants be distributed through the thickness of the nth layer as accepted throughout this paper

$$\Xi^{(n)} = \sum_{i_n} L^{(n)i_n} \Xi^{(n)i_n}, \quad \theta_3^{[n-1]} \le \theta_3 \le \theta_3^{[n]}, \tag{28}$$

$$\Xi^{(n)} = [C_{ijkl}^{(n)}, e_{ijk}^{(n)}, \gamma_{ij}^{(n)}, \in_{ij}^{(n)}, r_i^{(n)}, \rho^{(n)}, c_{\mathrm{V}}^{(n)}],$$

where $\Xi^{(n)i_n} = \Xi^{(n)}(\theta_3^{(n)i_n})$ are the values of material constants on SaS of the nth layer.

Analytical solution for layered composite cylindrical shell

In this section, we study a layered composite cylindrical shell with embedded piezoelectric layers subjected to thermal and electro-mechanical loads. The boundary conditions for the simply supported cylindrical shell with electrically grounded edges maintained at the reference temperature are written as

$$\Theta^{(n)} = \varphi^{(n)} = \sigma_{11}^{(n)} = u_2^{(n)} = u_3^{(n)} = 0 \ \text{at} \ \theta_1 = 0 \ \text{and} \ \theta_1 = L, \tag{29}$$

where θ_1 is the longitudinal coordinate; L is the length of the shell. To satisfy the boundary conditions (29), we search the analytical solution by a method of the double Fourier series expansion

$$\Theta^{(n)i_n} = \sum_{r=1}^{\infty}\sum_{s=0}^{\infty}\Theta_{rs}^{(n)i_n}\sin\frac{r\pi\theta_1}{L}\cos s\theta_2, \tag{30}$$

$$\varphi^{(n)i_n} = \sum_{r=1}^{\infty}\sum_{s=0}^{\infty}\varphi_{rs}^{(n)i_n}\sin\frac{r\pi\theta_1}{L}\cos s\theta_2, \tag{31}$$

$$u_1^{(n)i_n} = \sum_{r=1}^{\infty}\sum_{s=0}^{\infty}u_{1rs}^{(n)i_n}\cos\frac{r\pi\theta_1}{L}\cos s\theta_2, \tag{32}$$

$$u_2^{(n)i_n} = \sum_{r=1}^{\infty}\sum_{s=0}^{\infty}u_{2rs}^{(n)i_n}\sin\frac{r\pi\theta_1}{L}\sin s\theta_2, \tag{33}$$

$$u_3^{(n)i_n} = \sum_{r=1}^{\infty}\sum_{s=0}^{\infty}u_{3rs}^{(n)i_n}\sin\frac{r\pi\theta_1}{L}\cos s\theta_2, \tag{34}$$

where θ_2 is the circumferential coordinate; *r, s* are the wave numbers. The external electromechanical loads are also expanded in double Fourier series.

Substituting formula (30) in a variational equation of the heat conduction theory [18], we obtain the systems of linear algebraic equations in terms of temperatures $\Theta_{rs}^{(n)i_n}$ of order *K*, where $K = \sum_n I_n - N + 1$. Therefore, the temperatures of SaS can be found using the method of Gaussian elimination. Substituting then (31) – (34) in a variational equation of the thermopiezoelectric shell theory [18], one obtains the systems of linear algebraic equations in terms of $\varphi_{rs}^{(n)i_n}$, $u_{1rs}^{(n)i_n}$, $u_{2rs}^{(n)i_n}$ and $u_{3rs}^{(n)i_n}$ of order 4*K*, in which the temperatures of SaS $\Theta_{rs}^{(n)i_n}$ are known. These linear systems are solved again through the method of Gaussian elimination.

The described algorithm was performed with the Symbolic Math Toolbox, which incorporates symbolic computations into the numeric environment of MATLAB. This permits the obtaining of analytical solutions for layered composite cylindrical shells with piezoelectric layers in the framework of the SaS thermoelectroelastic shell formulation, which asymptotically approach the 3D exact solutions of thermopiezoelectricity as the number of SAS of the *n*th layer I_n tends to infinity.

Numerical examples

We consider a three-layer symmetric cross-ply cylindrical shell with the stacking sequence [90/0/90] composed of the graphite-epoxy composite and covered with two piezoelectric PVDF layers on its bottom and top surfaces. Thus, the hybrid five-layer cylindrical shell [PVDF/90/0/90/PVDF] with ply thicknesses $[3h_0/8h_0/8h_0/8h_0/3h_0]$ is studied, where $h_0 = h/30$. The material properties of the PVDF polarized in the thickness direction are taken to be [14]:

$$E_1 = E_2 = E_3 = 2\text{ GPa},\quad \nu_{12} = \nu_{23} = \nu_{31} = 1/3,$$

$$\alpha_{11} = \alpha_{22} = \alpha_{33} = 120\times10^{-6}\,1/\text{K},\quad k_{11} = k_{22} = k_{33} = 0.24\text{ W/mK},$$

$$d_{311} = 3\times10^{-12}\text{ m/V},\quad d_{322} = 23\times10^{-12}\text{ m/V},\quad d_{333} = -30\times10^{-12}\text{ m/V},$$

$$\in_{11} = \in_{22} = 3.078\times10^{-11}\text{ F/m},\quad \in_{33} = 3.141\times10^{-11}\text{ F/m},\quad r_3 = -27\times10^{-6}\text{ C/m}^2\text{K},$$

where E_i are the elastic moduli; ν_{ij} are the Poisson's ratios; α_{ij} are the thermal coefficients of expansion; d_{ijk} are the piezoelectric moduli. The material properties of the graphite-epoxy composite are chosen as follows [15]:

$$E_{\mathrm{L}} = 172.5\,\mathrm{GPa},\ \ E_{\mathrm{T}} = 6.9\,\mathrm{GPa},\ \ G_{\mathrm{LT}} = 3.45\,\mathrm{GPa},\ \ G_{\mathrm{TT}} = 1.38\,\mathrm{GPa},\ \ \nu_{\mathrm{LT}} = \nu_{\mathrm{TT}} = 0.25,$$

$$\alpha_{\mathrm{L}} = 0.57\times10^{-6}\ 1/\mathrm{K},\ \ \alpha_{\mathrm{T}} = 35.6\times10^{-6}\ 1/\mathrm{K},\ \ k_{\mathrm{L}} = 36.42\ \mathrm{W/mK},\ \ k_{\mathrm{T}} = 0.96\ \mathrm{W/mK},$$

$$\in_{\mathrm{L}} = 3.095\times10^{-11}\ \mathrm{F/m},\quad \in_{\mathrm{T}} = 2.653\times10^{-11}\ \mathrm{F/m},$$

where L and T denote the fiber and transverse directions. To evaluate the entropy, we accept $\rho = 1780\ \mathrm{kg/m^3}$, $c_{\mathrm{v}} = 1400\ \mathrm{J/kgK}$ and $\rho = 1800\ \mathrm{kg/m^3}$, $c_{\mathrm{v}} = 900\ \mathrm{J/kgK}$ for the PVDF and graphite-epoxy, respectively.

The shell is subjected to sinusoidally distributed temperature loading on the top surface, whereas the bottom surface is maintained at the reference temperature. The bottom and top surfaces are electroded and grounded. Therefore, the boundary conditions can be written as

$$\Theta^{+} = \Theta_0 \sin\frac{\pi\theta_1}{L},\quad \varphi^{+} = \sigma_{13}^{+} = \sigma_{23}^{+} = \sigma_{33}^{+} = 0,$$

$$\Theta^{-} = \varphi^{-} = \sigma_{13}^{-} = \sigma_{23}^{-} = \sigma_{33}^{-} = 0, \tag{35}$$

where $\Theta_0 = 1\mathrm{K}$ and $T_0 = 293\mathrm{K}$. The geometric parameters of the shell are chosen to be $R = 1\mathrm{m}$ and $L = 4\mathrm{m}$, where R is the radius of the middle surface. It is assumed that the interfaces between the piezoelectric layers and the substrate are electroded and grounded.

To compare the derived results with the 3D exact solution of thermoelectroelasticity [15], we introduce dimensionless variables at crucial points as follows:

$$\overline{\Theta} = \Theta(L/2, z)/\Theta_0,\quad \overline{\varphi} = 10^3 d_{\mathrm{r}}\varphi(L/2, z)/h\alpha_{\mathrm{r}}\Theta_0,$$

$$\overline{u}_1 = 100u_1(0,z)/R\alpha_{\mathrm{r}}\Theta_0,\ \ \overline{u}_3 = 10u_3(L/2,z)/R\alpha_{\mathrm{r}}\Theta_0,$$

$$\overline{q}_3 = 100hq_3(L/2, z)/k_{\mathrm{r}}\Theta_0,\quad \overline{\eta} = 10^{-3}\eta(L/2, z)/E_{\mathrm{r}}\alpha_{\mathrm{r}}^2\Theta_0,$$

$$\overline{\sigma}_{13} = 10S\sigma_{13}(0,z)/E_{\mathrm{r}}\alpha_{\mathrm{r}}\Theta_0,\ \ \overline{\sigma}_{33} = 10S\sigma_{33}(L/2,z)/E_{\mathrm{r}}\alpha_{\mathrm{r}}\Theta_0,$$

where $z = \theta_3/h$ is the dimensionless thickness coordinate; $S = R/h$ is the slenderness ratio; $E_{\mathrm{r}} = 6.9$ GPa, $\alpha_{\mathrm{r}} = 35.6\times10^{-6}\ 1/\mathrm{K}$, $k_{\mathrm{r}} = 36.42$ W/mK and $d_{\mathrm{r}} = 30\times10^{-12}$ m/V are the representative moduli of the shell.

Figures 2, 3 display the distributions of the temperature, electric potential, displacements, heat flux, entropy and stresses through the thickness of the hybrid layered cylindrical shell for different values of the slenderness ratio employing seven SaS for each layer. A comparison with the 3D exact solution [15] is also presented. These results demonstrate convincingly the high potential of the developed SaS formulation because the boundary conditions on bottom and top surfaces of the shell for transverse stresses and the continuity conditions for the heat flux and transverse stresses at interfaces are satisfied exactly.

Next, we study a simply supported metal-ceramic cylindrical shell covered with the graphite-epoxy layer and PVDF at the bottom. Therefore, we deal here with a hybrid three-layer shell [PVDF/Graphite-Epoxy/Metal-Ceramic] with ply thicknesses [0.1*h*/0.1*h*/0.8*h*]. The fibers of the graphite-epoxy composite are oriented in the axial

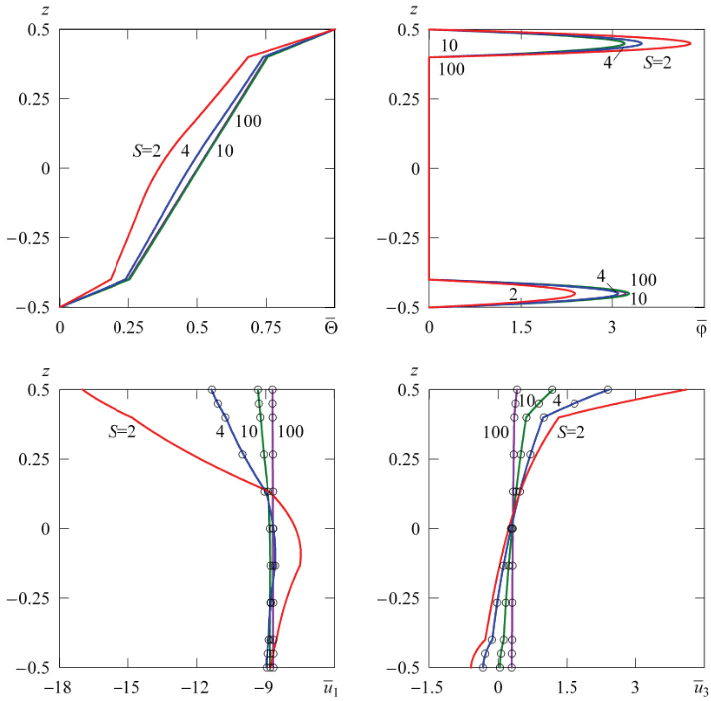

Fig. 2. Through-thickness distributions of the temperature, electric potential and displacements for a hybrid five-layer cylindrical shell: SaS formulation for seven SaS inside each layer and 3D exact solution (○) [15]

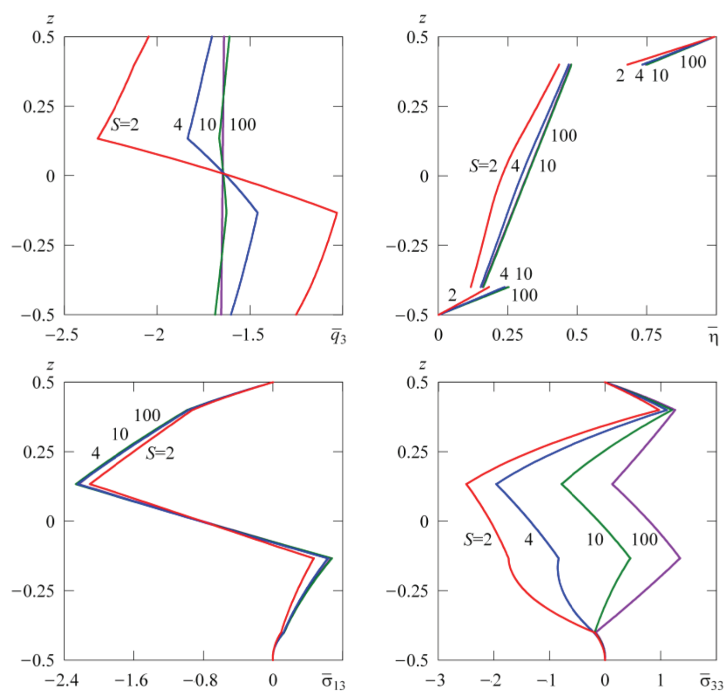

Fig. 3. Through-thickness distributions of the heat flux, entropy and stresses for a hybrid five-layer cylindrical shell: SaS formulation for seven SaS inside each layer

direction. The material properties of the graphite-epoxy and PVDF are presented in a previous example. The metal-ceramic shell is made of the two-phase composite. The metal phase is aluminum with $E_{\mathrm{m}} = 7 \times 10^{10}\,\mathrm{Pa}$, $\nu_{\mathrm{m}} = 0.3$, $\alpha_{\mathrm{m}} = 23.4 \times 10^{-6}\,1/\mathrm{K}$, $k_{\mathrm{m}} = 233\,\mathrm{W/mK}$, $\rho_{\mathrm{m}} = 2707\,\mathrm{kg/m^3}$ and $c_{\mathrm{m}} = 896\,\mathrm{J/kgK}$; the thermal barrier is a SiC ceramic with $E_{\mathrm{c}} = 38 \times 10^{10}\,\mathrm{Pa}$, $\nu_{\mathrm{c}} = 0.17$, $\alpha_{\mathrm{c}} = 4.3 \times 10^{-6}\,1/\mathrm{K}$, $k_{\mathrm{c}} = 65\,\mathrm{W/mK}$, $\rho_{\mathrm{c}} = 3100\,\mathrm{kg/m^3}$ and $c_{\mathrm{c}} = 670\,\mathrm{J/kgK}$. It is assumed that the material properties are varied through the thickness according to the rule of mixtures:

$$E = E_{\mathrm{m}} V_{\mathrm{m}} + E_{\mathrm{c}} V_{\mathrm{c}}, \quad \nu = \nu_{\mathrm{m}} V_{\mathrm{m}} + \nu_{\mathrm{c}} V_{\mathrm{c}}, \quad \alpha = \alpha_{\mathrm{m}} V_{\mathrm{m}} + \alpha_{\mathrm{c}} V_{\mathrm{c}},$$

$$k = k_{\mathrm{m}} V_{\mathrm{m}} + k_{\mathrm{c}} V_{\mathrm{c}}, \quad \rho c = \rho_{\mathrm{m}} c_{\mathrm{m}} V_{\mathrm{m}} + \rho_{\mathrm{c}} c_{\mathrm{c}} V_{\mathrm{c}}, \tag{36}$$

where V_{m} and V_{c} are the volume fractions of metal and ceramic phases defined as

$$V_{\mathrm{m}} = 1 - V_{\mathrm{c}}, \quad V_{\mathrm{c}} = \left[(z + 0.3)/0.8\right]^{\gamma}, \quad z \in [-0.3,\ 0.5], \tag{37}$$

where γ is the material gradient index; $z = \theta_3 / h$ is the dimensionless thickness coordinate.

Here, we study a cylindrical shell subjected to sinusoidally distributed temperature loading on the top surface and consider the following boundary conditions:

$$\Theta^+ = \Theta_0 \sin \frac{\pi \theta_1}{L} \cos 2\theta_2, \quad \varphi^+ = \sigma_{13}^+ = \sigma_{23}^+ = \sigma_{33}^+ = 0,$$

$$\Theta^- = 0, \quad D_3^- = \sigma_{13}^- = \sigma_{23}^- = \sigma_{33}^- = 0, \tag{38}$$

where $\Theta_0 = 1\,\mathrm{K}$ and $T_0 = 293\,\mathrm{K}$. The interface between PVDF and graphite-epoxy is electroded and grounded.

To analyze the obtained results efficiently, we introduce dimensionless variables at crucial points as functions of the dimensionless thickness coordinate $z = \theta_3 / h$ as

$$\overline{\Theta} = \Theta(L/2, 0, z)/\Theta_0, \quad \overline{\varphi} = d_{\mathrm{r}} \varphi(L/2, 0, z)/h\alpha_{\mathrm{r}}\Theta_0,$$

$$\overline{u}_1 = 10^{-4} u_1(0, 0, z)/R\alpha_{\mathrm{r}}\Theta_0, \quad \overline{u}_3 = 10^{-5} u_3(L/2, 0, z)/R\alpha_{\mathrm{r}}\Theta_0,$$

$$\overline{\sigma}_{11} = 10^{-5} \sigma_{11}(L/2, 0, z)/E_{\mathrm{r}}\alpha_{\mathrm{r}}\Theta_0, \quad \overline{\sigma}_{22} = 10^{-5} \sigma_{22}(L/2, 0, z)/E_{\mathrm{r}}\alpha_{\mathrm{r}}\Theta_0,$$

$$\overline{\sigma}_{12} = 10^{-4} S\sigma_{12}(0, \pi/4, z)/E_{\mathrm{r}}\alpha_{\mathrm{r}}\Theta_0, \quad \overline{\sigma}_{13} = 10^{-3} S\sigma_{13}(0, 0, z)/E_{\mathrm{r}}\alpha_{\mathrm{r}}\Theta_0,$$

$$\overline{\sigma}_{23} = 10^{-3} S\sigma_{23}(L/2, \pi/4, z)/E_{\mathrm{r}}\alpha_{\mathrm{r}}\Theta_0, \quad \overline{\sigma}_{33} = 10^{-3} S\sigma_{33}(L/2, 0, z)/E_{\mathrm{r}}\alpha_{\mathrm{r}}\Theta_0, \quad S = R/h,$$

where E_{r} and α_{r} are the representative moduli taken from a previous example. The geometric parameters of the shell are chosen as $R = 1\,\mathrm{m}$ and $L = 4\,\mathrm{m}$.

Figures 4, 5 show the through-thickness distributions of the temperature, electric potential, displacements and stresses for different values of the slenderness ratio S and material gradient index $\gamma = 2$ using 13 SaS for each layer. These results demonstrate again the high potential of the developed SaS shell formulation, since the boundary conditions on the bottom and top surfaces and the continuity conditions at the interfaces for transverse stresses are satisfied properly.

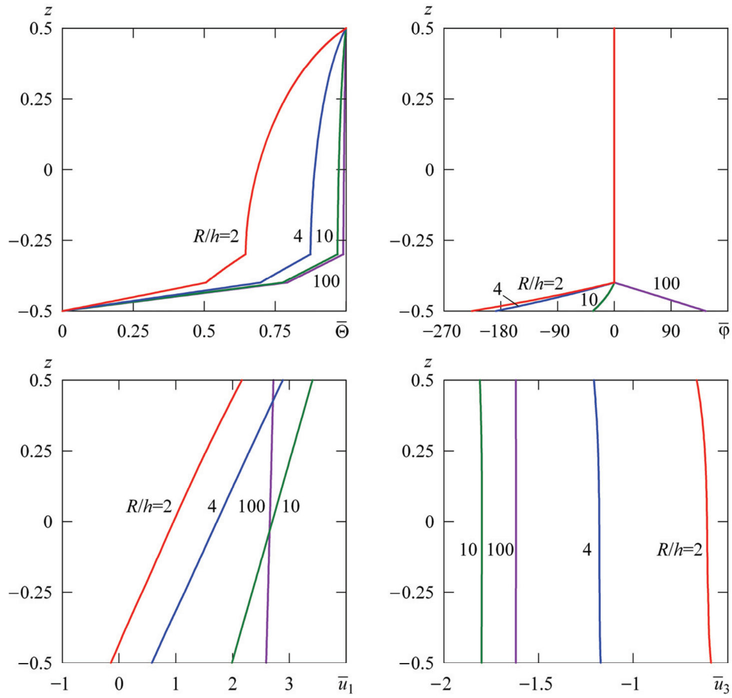

Fig. 4. Through-thickness distributions of the temperature, electric potential and displacements for a hybrid three-layer cylindrical shell: SaS formulation for $\gamma = 2$ and 13 SaS inside each layer

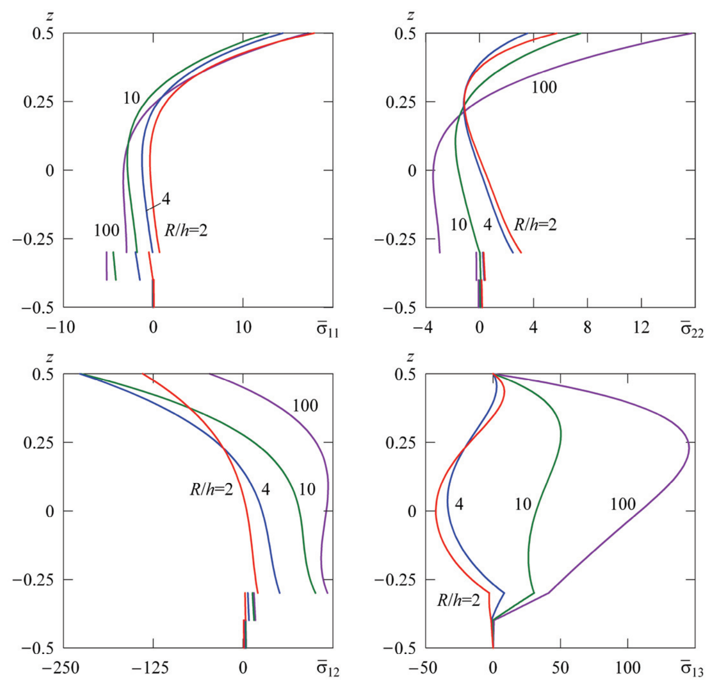

Fig. 5. Through-thickness distributions of stresses for a hybrid three-layer cylindrical shell: SaS formulation for $\gamma = 2$ and 13 SaS inside each layer (continued p. 317)

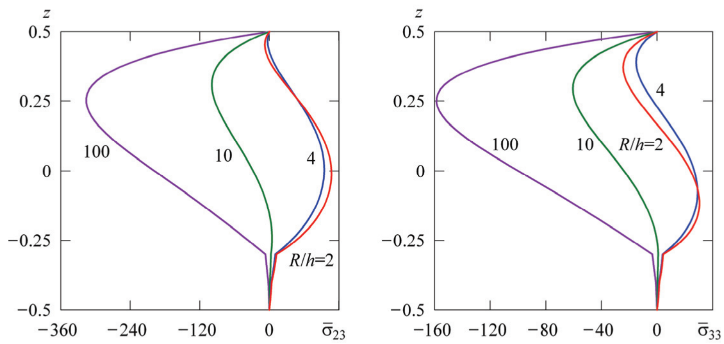

Fig. 5. Through-thickness distributions of stresses for a hybrid three-layer cylindrical shell: SaS formulation for $\gamma = 2$ and 13 SaS inside each layer

Conclusions

A robust SaS formulation for the coupled steady-state thermal stress analysis of layered piezoelectric shells has been proposed. It is based on a concept of SaS located at Chebyshev polynomial nodes throughout the layers and interfaces as well. As a result, the developed SaS formulation makes it possible to obtain the Ritz solutions for hybrid layered cylindrical shells with piezoelectric sensors and actuators with a prescribed accuracy, which can asymptotically approach the 3D exact solutions of thermopiezoelectricity as the number of SaS goes to infinity.

This work was supported by the Russian Science Foundation (Grant No. 18-19-00092).

References

1. Wu C.P., Chiu K.H., Wang Y.M. A review on the three-dimensional analytical approaches of multilayered and functionally graded piezoelectric plates and shells, *Computers, Materials & Continua*, 2008, vol. 8, pp. 93-132.

2. Wu C.P., Liu Y.C. A review of semi-analytical numerical methods for laminated composite and multilayered functionally graded elastic/piezoelectric plates and shells, *Composite Structures*, 2016, vol. 147, pp. 1-15.

3. Dube G.P., Kapuria S., Dumir P.C. Exact piezothermoelastic solution of simply-supported orthotropic flat panel in cylindrical bending, *International Journal of Mechanical Sciences*, 1996, vol. 38, pp. 1161-1177.

4. Shang F., Wang Z., Li Z. Analysis of thermally induced cylindrical flexure of laminated plates with piezoelectric layers, *Composites Part B: Engineering*, 1997, vol. 28, pp. 185-193.

5. Ootao Y., Tanigawa Y. Three-dimensional transient piezothermoelasticity for a rectangular composite plate composed of cross-ply and piezoelectric laminae, *International Journal of Engineering Science*, 2000, vol. 38, pp. 47-71.

6. Zhang C., Di S., Zhang N. A new procedure for static analysis of thermo-electric laminated composite plates under cylindrical bending, *Composite Structures*, 2002, vol. 56, pp. 131-140.

7. Zhang C., Cheung Y.K., Di S., Zhang N. The exact solution of coupled thermoelectroelastic behavior of piezoelectric laminates, *Composite Structures*, 2002, vol. 80, pp. 1201-1212.

8. Xu K., Noor A.K., Tang Y.Y. Three-dimensional solutions for coupled thermoelectroelastic response of multilayered plates, *Computer Methods in Applied Mechanics and Engineering*, 1995, vol. 126, pp. 355-371.

9. Tarn J.Q. A state space formalism for piezothermoelasticity, *International Journal of Solids and Structures*, 2002, vol. 39, pp. 5173-5184.

10. Tarn J.Q., Chang H.H. A refined state space formalism for piezothermoelasticity, *International Journal of Solids and Structures*, 2008, vol. 45, pp. 3021-3032.

11. Vel S.S., Batra R.C. Generalized plane strain thermopiezoelectric analysis of multilayered plates, *Journal of Thermal Stresses*, 2003, vol. 26, pp. 353-377.

12. Zhong Z., Shang E.T. Exact analysis of simply supported functionally graded piezothermoelectric plates, *Journal of Intelligent Material Systems and Structures*, 2005, vol. 16, pp. 643-651.

13. Xu K., Noor A.K. Three-dimensional analytical solutions for coupled thermoelectroelastic response of multilayered cylindrical shells, *AIAA Journal*, 1996, vol. 34, pp. 802-810.

14. Kapuria S., Dumir P.C., Sengupta S. An exact axisymmetric solution for a simply supported piezoelectric cylindrical shell, *Archive of Applied Mechanics*, 1997, vol. 67, pp. 260-273.

15. Kapuria S., Sengupta S., Dumir P.C. Three-dimensional solution for a hybrid cylindrical shell under axisymmetric thermoelectric load, *Archive of Applied Mechanics*, 1997, vol. 67, pp. 320-330.

16. Cheng Z.Q., Batra R.C. Three-dimensional asymptotic scheme for piezothermoelastic laminates, *Journal of Thermal Stresses*, 2000, vol. 23, pp. 95-110.

17. Kulikov G.M., Plotnikova S.V. Exact 3D thermoelectroelastic analysis of piezoelectric plates through a sampling surfaces method, *Mechanics of Advanced Materials and Structures*, 2015, vol. 22, pp. 33-43.

18. Kulikov G.M., Mamontov A.A., Plotnikova S.V. Coupled thermoelectroelastic stress analysis of piezoelectric shells, *Composite Structures*, 2015, vol. 124, pp. 65-76.

19. Kulikov G.M., Plotnikova S.V. An analytical approach to three-dimensional coupled thermoelectroelastic analysis of functionally graded piezoelectric plates, *Journal of Intelligent Material Systems and Structures*, 2017, vol. 28, pp. 435-450.

20. Kulikov G.M., Plotnikova S.V. Advanced formulation for laminated composite shells: 3D stress analysis and rigid-body motions, *Composite Structures*, 2013, vol. 95, pp. 236-246.

21. Kulikov G.M. Refined global approximation theory of multilayered plates and shells, *Journal of Engineering Mechanics*, 2001, vol. 127, pp. 119-125.

22. Kulikov G.M., Carrera E. Finite deformation higher-order shell models and rigid-body motions, *International Journal of Solids and Structures*, 2008, vol. 45, pp. 3153-3172.

23. Kulikov G.M., Plotnikova S.V. Solution of static problems for a three-dimensional elastic shell, *Doklady Physics*, 2011, vol. 56, no. 8, pp. 448-451.

24. Burden R.L., Faires J.D. *Numerical Analysis*, (9th Edition), Brooks/Cole, Cengage Learning, Boston, USA, 2010, 872 p.

25. Kulikov G.M., Plotnikova S.V. [Solution of three-dimensional problems of thermoelasticity for laminated shells made of functionally graded materials], *Transactions of the Tambov State Technical University*, 2015, vol. 21, no. 1, pp. 185-190. (In Russ., abstract in Eng.)

26. Kulikov G.M., Carrera E., Plotnikova S.V. Hybrid-mixed quadrilateral element for laminated plates composed of functionally graded materials, *Advanced Materials & Technologies*, 2017, no. 1, pp. 44-55. doi: 10.17277/amt.2017.01.pp.044-055

Связанный термоэлектромеханический анализ гибридных слоистых цилиндрических оболочек с пьезоэлектрическими сенсорами и актуаторами

Г. М. Куликов, Н. П. Меркушева, М. Г. Куликов, С. В. Плотникова

Научно-исследовательская лаборатория «Механика интеллектуальных материалов и конструкций», gmkulikov@mail.ru;
ФГБОУ ВО «ТГТУ», г. Тамбов, Россия

Ключевые слова: слоистая пьезоэлектрическая оболочка, термопьезоэлектричество, трехмерный анализ напряжений, метод отсчетных поверхностей.

Аннотация: Данная статья посвящена реализации метода отсчетных поверхностей (SaS метод) для решения трехмерных связанных задач для слоистых пьезоэлектрических оболочек, подверженных температурным и электромеханическим воздействиям. SaS метод основан на выборе внутри *n*-го слоя I_n отсчетных поверхностей параллельных срединной поверхности, чтобы ввести температуры, электрические потенциалы и перемещения этих поверхностей в качестве искомых функций. Такой выбор неизвестных с последующим использованием полиномов Лагранжа степени $I_n - 1$ в аппроксимациях температуры, электрического потенциала, перемещений и механических параметров материала по толщине слоя приводит к эффективной модели термопьезоэлектрической оболочки. Внутренние SaS расположены внутри каждого слоя в узловых точках полинома Чебышева, что позволяет равномерно минимизировать погрешность приближения полиномами Лагранжа высокого порядка. В результате SaS метод может быть применен к построению аналитических решений для гибридных слоистых цилиндрических оболочек с пьезоэлектрическими сенсорами и актуаторами, которые асимптотически приближаются к точным решениям термопьезоэлектричества при стремлении числа отсчетных поверхностей I_n к бесконечности.

Список литературы

1. Wu, C. P. A review on the three-dimensional analytical approaches of multilayered and functionally graded piezoelectric plates and shells / C. P. Wu, K. H. Chiu, Y. M. Wang // Computers, Materials & Continua. – 2008. – Vol. 8. – P. 93 – 132.

2. Wu, C. P. A review of semi-analytical numerical methods for laminated composite and multilayered functionally graded elastic/piezoelectric plates and shells / C. P. Wu, Y. C. Liu // Composite Structures. – 2016. – Vol. 147. – P. 1 – 15.

3. Dube, G. P. Exact piezothermoelastic solution of simply-supported orthotropic flat panel in cylindrical bending / G. P. Dube, S. Kapuria, P. C. Dumir // International Journal of Mechanical Sciences. – 1996. – Vol. 38. – P. 1161 – 1177.

4. Shang, F. Analysis of thermally induced cylindrical flexure of laminated plates with piezoelectric layers / F. Shang, Z. Wang, Z. Li // Composites Part B: Engineering. – 1997. – Vol. 28. – P. 185 – 193.

5. Ootao, Y. Three-dimensional transient piezothermoelasticity for a rectangular composite plate composed of cross-ply and piezoelectric laminae / Y. Ootao, Y. Tanigawa // International Journal of Engineering Science. – 2000. – Vol. 38. – P. 47 – 71.

6. Zhang, C. A new procedure for static analysis of thermo-electric laminated composite plates under cylindrical bending / C. Zhang, S. Di, N. Zhang // Composite Structures. – 2002. – Vol. 56. – P. 131 – 140.

7. Zhang, C. The exact solution of coupled thermoelectroelastic behavior of piezoelectric laminates / C. Zhang, Y. K. Cheung, S. Di, N. Zhang // Composite Structures. – 2002. – Vol. 80. – P. 1201 – 1212.

8. Xu, K. Three-dimensional solutions for coupled thermoelectroelastic response of multilayered plates / K. Xu, A. K. Noor, Y. Y. Tang // Computer Methods in Applied Mechanics and Engineering. – 1995. – Vol. 126. – P. 355 – 371.

9. Tarn, J. Q. A state space formalism for piezothermoelasticity / J. Q. Tarn // International Journal of Solids and Structures. – 2002. – Vol. 39. – P. 5173 – 5184.

10. Tarn, J. Q. A refined state space formalism for piezothermoelasticity / J. Q. Tarn, H. H. Chang // International Journal of Solids and Structures. – 2008. – Vol. 45. – P. 3021 – 3032.

11. Vel, S. S. Generalized plane strain thermopiezoelectric analysis of multilayered plates / S. S. Vel, R. C. Batra // Journal of Thermal Stresses. – 2003. – Vol. 26. – P. 353 – 377.

12. Zhong, Z. Exact analysis of simply supported functionally graded piezothermoelectric plates / Z. Zhong, E. T. Shang // Journal of Intelligent Material Systems and Structures. – 2005. – Vol. 16. – P. 643 – 651.

13. Xu, K. Three-dimensional analytical solutions for coupled thermoelectroelastic response of multilayered cylindrical shells / K. Xu, A. K. Noor // AIAA Journal. – 1996. – Vol. 34. – P. 802 – 810.

14. Kapuria, S. An exact axisymmetric solution for a simply supported piezoelectric cylindrical shell / S. Kapuria, P. C. Dumir, S. Sengupta // Archive of Applied Mechanics. – 1997. – Vol. 67. – P. 260 – 273.

15. Kapuria, S. Three-dimensional solution for a hybrid cylindrical shell under axisymmetric thermoelectric load / S. Kapuria, S. Sengupta, P. C. Dumir // Archive of Applied Mechanics. – 1997. – Vol. 67. – P. 320 – 330.

16. Cheng, Z. Q. Three-dimensional asymptotic scheme for piezothermoelastic laminates / Z. Q. Cheng, R. C. Batra // Journal of Thermal Stresses. – 2000. – Vol. 23. – P. 95 – 110.

17. Kulikov, G. M. Exact 3D thermoelectroelastic analysis of piezoelectric plates through a sampling surfaces method / G. M. Kulikov, S. V. Plotnikova // Mechanics of Advanced Materials and Structures. – 2015. – Vol. 22. – P. 33 – 43.

18. Kulikov, G. M. Coupled thermoelectroelastic stress analysis of piezoelectric shells / G. M. Kulikov, A. A. Mamontov, S. V. Plotnikova // Composite Structures. – 2015. – Vol. 124. – P. 65 – 76.

19. Kulikov, G. M. An analytical approach to three-dimensional coupled thermoelectroelastic analysis of functionally graded piezoelectric plates / G. M. Kulikov, S. V. Plotnikova // Journal of Intelligent Material Systems and Structures. – 2017. – Vol. 28. – P. 435 – 450.

20. Kulikov, G. M. Advanced formulation for laminated composite shells: 3D stress analysis and rigid-body motions / G. M. Kulikov, S. V. Plotnikova // Composite Structures. – 2013. – Vol. 95. – P. 236 – 246.

21. Kulikov, G. M. Refined global approximation theory of multilayered plates and shells / G. M. Kulikov // Journal of Engineering Mechanics. – 2001. – Vol. 127. – P. 119 – 125.

22. Kulikov, G. M. Finite deformation higher-order shell models and rigid-body motions / G. M. Kulikov, E. Carrera // International Journal of Solids and Structures. – 2008. – Vol. 45. – P. 3153 – 3172.

23. Куликов, Г.М. Решение задачи статики для упругой оболочки в пространственной постановке / Г. М. Куликов, С.В. Плотникова // Докл. академии наук. – 2011. – Т. 439, № 5. – С. 613 – 616.

24. Burden, R. L. Numerical Analysis / R. L. Burden, J. D. Faires. – 9th Edition. – Brooks/Cole, Cengage Learning, Boston, USA, 2010. – 872 p.

25. Куликов Г. М. Решение трехмерных задач термоупругости для слоистых оболочек из функциональных материалов / Г. М. Куликов, С. В. Плотникова // Вестн. Тамб. гос. техн. ун-та. – 2015. – Т. 21, № 1. – С. 185 – 190.

26. Kulikov, G. M. Hybrid-mixed quadrilateral element for laminated plates composed of functionally graded materials / G. M. Kulikov, E. Carrera, S. V. Plotnikova // Advanced Materials & Technologies. – 2017. – No. 1. – P. 44 – 55. doi: 10.17277/amt.2017.01.pp.044-055

Verwandte thermoelektromechanische Analyse von Hybrid-Zylinderschalen mit piezoelektrischen Sensoren und Aktuatoren

Zusammenfassung: Dieser Artikel befasst sich mit der Implementierung der Referenzoberflächenmethode (SaS-Methode) zur Lösung dreidimensional gekoppelter Probleme für geschichtete piezoelektrische Schalen, die Temperatur- und elektromechanischen Effekten ausgesetzt sind. Das SaS-Verfahren basiert auf der Auswahl von Bezugsflächen parallel zur mittleren Oberfläche innerhalb der n-ten Schicht I_n, um Temperaturen, elektrische Potentiale und Verschiebungen dieser Oberflächen als gewünschte Funktionen einzuführen. Eine solche Auswahl von Unbekannten mit der anschließenden Verwendung von Lagrange-Polynomen des Grades $I_n - 1$ in Approximationen von Temperatur, elektrischem Potential, Verschiebungen und mechanischen Parametern des Materials über die Schichtdicke führt zu einem effektiven Modell einer thermopiezoelektrischen Hülle. Interne SaSs befinden sich in jeder Schicht an den Knotenpunkten des Chebyshev-Polynoms, wodurch der Approximationsfehler von Lagrange-Polynomen hoher Ordnung gleichmäßig minimiert werden kann. Infolgedessen kann die SaS-Methode auf die Konstruktion von analytischen Lösungen für Hybridschicht-Zylinderschalen mit piezoelektrischen Sensoren und Aktuatoren angewendet werden, die sich asymptotisch den exakten Lösungen der Thermo-Piezoelektrizität nähern, wenn die Anzahl der Bezugsflächen I_n gegen unendlich tendiert.

Analyse associée thermoélectromécanique des coques cylindriques en couches hybrides avec capteurs et actionneurs piézoélectriques

Résumé: L’article est consacré à la mise en œuvre de la méthode SaS pour résoudre des problèmes liés 3D pour des couches piézoélectriques soumises à des influences thermiques et électromécaniques. La méthode SaS est basée sur la sélection à l'intérieur de la nième couche de surfaces de référence parallèles à la surface médiane pour introduire des températures, des potentiels électriques et le déplacement de ces surfaces en qualité des fonctions souhaitées. Un tel choix d'inconnues, suivie de l'utilisation des polynômes de Lagrange de degré dans les approximations de la température, du potentiel électrique, des déplacements et des paramètres mécaniques du matériau sur l'épaisseur de la couche, aboutit à un modèle efficace de la coque thermopyézoélectrique. Les SaS internes sont situés à l'intérieur de chaque couche aux points nodaux du polynôme de Chebyshev, ce qui permet de minimiser uniformément l'erreur d'approximation des polynômes de Lagrange d'ordre élevé. En conséquence, la méthode SaS peut être appliquée à la construction de solutions analytiques pour des coques cylindriques en couches hybrides avec des capteurs piézoélectriques et des actuateurs qui se rapprochent asymptotiquement des solutions précises de thermopyézoélectricité tout en cherchant le nombre de surfaces de référence à l'infini.

Авторы: ***Куликов Геннадий Михайлович*** – доктор физико-математических наук, профессор, заведующий научно-исследовательской лабораторией «Механика интеллектуальных материалов и конструкций»; ***Меркушева Наталия Павловна*** – инженер научно-исследовательской лаборатории «Механика интеллектуальных материалов и конструкций»; ***Куликов Михаил Геннадьевич*** – кандидат технических наук, старший научный сотрудник научно-исследовательской лаборатории «Механика интеллектуальных материалов и конструкций»; ***Плотникова Светлана Валерьевна*** – доктор технических наук, ведущий научный сотрудник научно-исследовательской лаборатории «Механика интеллектуальных материалов и конструкций», ФГБОУ ВО «ТГТУ», г. Тамбов, Россия.

Рецензент: ***Нахман Александр Давидович*** – кандидат физико-математических наук, доцент кафедры «Высшая математика», ФГБОУ ВО «ТГТУ», г. Тамбов, Россия.